Research Article

SOHAG JOURNAL OF SCIENCES

https://doi.org/10.21608/sjsci.2024.247829.1146

Impact of Cold Atmospheric Plasma Treatment Duration on Distilled Water Physicochemical Characteristics

Ghada Abd El-Reda[1,2*], Manal A. M. Mahmoud[3], Mohamed Khalaf [2], Ayman A. Saber[2], F. M. El-Hossary[2]

[1] *Physics Department, Faculty of Science, Assiut University, Assiut 71516, Egypt*
[2] *Physics Department, Faculty of Science, Sohag University, Sohag 82524, Egypt*
[3] *Animal Hygiene and Environmental Pollution Department, Faculty of Veterinary Medicine, Assiut University, Assiut 71526, Egypt*
**Email: ghadaabdelreda@aun.edu.eg*

Received: 13th November 2023 **Revised:** 11th December 2023 **Accepted:** 15th January 2024
Published online: 21st February 2024

Abstract: A thrilling technological advance is plasma-activated water, or PAW, with potential applications in various fields. Nevertheless, additional research is required for a comprehensive understanding of its physicochemical properties and how they can be optimized for specific applications. The current study employed different analytical methods to examine the effects of varying exposure durations of PAW generated using air as a working gas (ranging from 0 to 15 minutes) on the temperature, electric conductivity (EC), contact angle, pH, H_2O_2, and NO^-_2 measurements of PAW. Additionally, the study explored the effects of PAW storage at a temperature of -20°C and the stability of pH, hydrogen peroxide (H_2O_2), and nitrite anion (NO^-_2) levels over a period of up to 20 days after its production. The results clarified that the PAW contains reactive oxygen (ROS) and nitrogen species (RNS), specifically H_2O_2, and NO^-_2, which can be stored for at least over 20 days at -20°C without significant changes in concentration. Plasma treatment increases the conductivity of water over time, and the pH decreases with prolonged exposure. The study provides valuable insights into the diverse applications of PAW in distinct research and industrial domains.
Keywords: Plasma-activated water (PAW), time of exposure, storage effect, physicochemical attributes.

1. Introduction

PAW is emerging as an innovative technology that has received significant attention in recent years due to its distinctive properties and potential applications in various fields, including biomedicine, agriculture, and environmental sciences. In biomedicine, PAW has been studied for its potential as an antimicrobial agent against drug-resistant bacteria, viruses, and fungi. PAW has also been shown to have the potential to promote wound healing, reduce inflammation, and as a cancer therapy [1]. In agriculture, PAW has been investigated for its potential to improve crop growth and disease resistance and treat plant pathogens [2]. Additionally, PAW has been shown to have potential in environmental applications, such as the removal of pollutants and the treatment of wastewater [3]. The physical and chemical properties of PAW are crucial factors that determine its effectiveness in different applications [1], [4-11].

PAW is produced by exposing water to plasma, which is a partially ionized gas consisting of a complex mixture of ions, electrons, and neutral species. PAW could be generated using various gases such as air [12], oxygen, helium [11], argon, and nitrogen. The composition of the gas used for PAW generation can affect the properties and formation of reactive species in plasma. Among the commonly used gases, air is preferred due to its availability and low cost [13-18]. During air plasma treatment, various reactive species such as H_2O_2, NO_2, and OH radicals are formed, which are responsible for the antimicrobial and other beneficial properties of PAW. Several factors influence PAW properties, including plasma characteristics like the input power amount, rate of gas flow, and treatment duration. Water quality, including pH, conductivity (EC), and impurities, can also impact the stability and composition of PAW. Furthermore, the plasma source type plays a role in PAW properties, with different sources producing varying concentrations and types of reactive species [19].

Recently, the potential applications of PAW generated using air as a working gas in various fields have attracted considerable attention. However, a limited understanding of the physical and chemical properties of PAW generated using air as a working gas has hindered the development of technologies utilizing this substance. One of the critical factors that influence the characteristics of PAW is exposure time to plasma. Understanding the impact of exposure time on the properties of PAW is crucial to developing more applications that are effective across various fields. To address this research gap, this study employed different analytical methods to examine the effects of varying exposure durations of PAW generated using air as a working gas (ranging from 0 to 15 minutes) on the temperature, EC, contact angle, pH, H_2O_2, and RNS measurements of PAW. In addition, the study investigated the effects of PAW storage at a temperature of -20°C and the stability of pH, hydrogen peroxide, nitrate, and nitrite anion levels over a period of up to 20 days after its production. Limited information is currently available regarding the impact of storage conditions on PAW, making this research significant in terms of advancing our understanding of how to properly store and maintain the efficacy of this solution. The findings of this

study provided valuable insights into the physical and chemical properties of PAW, which can contribute to a better understanding of plasma-water interactions and enable innovation and development in this field.

2. Materials and Method

2.1. Cold atmospheric plasma (CAP) discharge device

The setup used in the experiments for plasma treating distilled water (DW) is depicted in Fig. 1. A high AC voltage (5 kV) was applied on a hollow needle stainless-steel electrode. The experimental plasma unit was assembled using a high-voltage power supply operating at a frequency of 50 kHz. This power source was attached to an electrode with a diameter of 1 mm and a surface area of 3 cm^2. DW was contained in a 100 ml plastic cup with Aluminum foil (0.1 mm thick, 7 mm wide, and 29 cm long) and was ring electrode wrapped around the plate tube. The spark discharge was obtained between the tip of the needle electrode and DW 5 mm apart. A photograph of spark plasma is shown in Fig 2.

PAW was produced by creating plasma at the water's surface, employing room-temperature atmospheric pressure air as the operational gas. 100 mL of DW was activated by plasma for different treatment times 1, 3, 5, 8, 10, 12, and 15 min to prepare. Then, 100 mL of PAW was divided into 2 mL Eppendorf tubes and kept in a -20 °C freezer until used for analysis, the remaining samples were thawed hygienically.

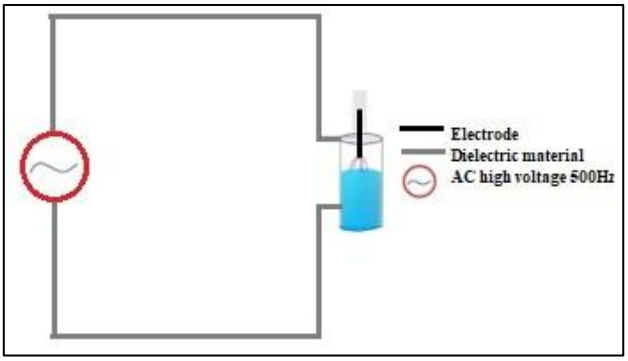

Figure 1: Water treatment experimental system set-up

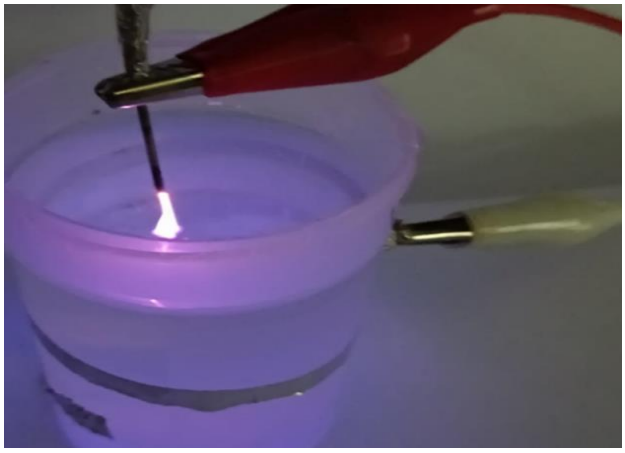

Figure 2: Photograph spark plasma

A two-channel digital oscilloscope analyzed the plasma reactor's high voltage and current waveforms. A high-voltage probe (1000:1) was employed and linked to a plasma electrode in parallel for voltage recording. The second channel was dedicated to a 100 Ohm resistor connected between the ground terminal and the ground electrode, enabling the detection of discharge current, as illustrated in Fig. 3. Optical emission data were acquired using a spectrometer connected to an optical fiber, positioned at a 1 cm distance from the plasma. This setup enabled the identification of species and recording of spectral features within the 300–900 nm range.

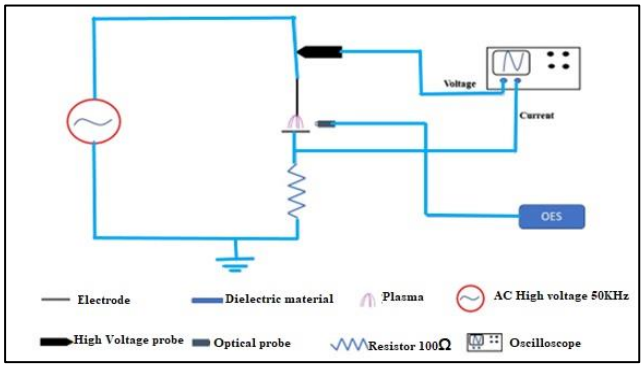

Figure 3: Schematic of electrical and optical measurements set-up.

2.2. Physicochemical measurement

The measurements were conducted promptly following the plasma treatment. In addition, they were measured at 10 and 20 days after storage at -20 °C.

2.2.1. PH, temperature, and electrical conductivity (EC)

Adwa waterproof pH-Temp tester AD14 and AD31 waterproof EC, TDS, and temperature testers (Adwa, Romania) were utilized to assess the DW's pH, temperature, and EC before and after the plasma activation. The temperature can be measured with a precision of 0.5°C within the range of –5°C to 60°C, pH within the range of 2 to 16 with an accuracy of up to 0.01, and EC within the range of 0 to 3120 µS/cm. An air conditioning system keeps the outside temperature of the hermetic container at 29°C during all treatments.

2.2.2. Contact Angle Measurement

The SEO Phoenix 300 contact angle analyzer was used to determine the contact angle between liquid droplets and glass. Following procedures published by Shaji et al. (Shaji et al., 2023), a simplified experimental arrangement was employed for drop shape analysis. Images of droplets containing 20 µL of PAW and DW on pristine glass microscope slides were taken for subsequent analysis. The contact angle measurements were conducted using the Surfaceware-8 image analysis software. Contact angle measurements were limited to room temperature only.

2.2.3. Hydrogen peroxide (H_2O_2)

The hydrogen peroxide (H_2O_2) was quantified using Biodiagnostic kits, Egypt, following the manufacturer procedures (Biodiagnostic, Dokki, Giza, Egypt, CAT. Number HP 25).

$$2H_2O_2 + DHBS + AAP \xrightarrow{HRP} Quinoneimine\ Dye + 4H_2O$$

With the existence of horseradish peroxidase (HRP), H_2O_2 reacts with 3,5-dichloro-2-hydroxybenzensulfonic (DHBS) acid and 4-aminophenazone (AAP) to produce a chromophore. The sample (A Sample) and standard (A Standard) were read against blank at 510 nm (OPTIZEN Alpha, K LAB CO.,LTD). Linearity up to 1.5 mM / L

$$H_2O_2 \text{ concentration (mM/L)} = \frac{A_{Sample}}{A_{standered}} \times 0.5$$

2.2.4. The nitrite (NO_2–)

Nitrites were quantified by colorimetric assay using Griess reagent (Biodiagnostic, Dokki, Giza, Egypt, CAT. Number TA 2533). The Griess reagent consists of two primary components. The first is sulphanilic acid, which reacts with nitrites to generate diazonium salt. The second component is naphthyl ethylenediamine dihydrochloride (NEDA), employed to create an azo dye agent in conjunction with the diazonium salt. The resulting azo dye agent exhibits a pink color with a characteristic absorbance at 540 nm (OPTIZEN Alpha, K LAB CO.,LTD)

$$\text{The total nitrite } (NO_2-) \text{ (µM/L)} = \frac{A_{\text{Sample}}}{A_{\text{standered}}} \times 50$$

2.2.5. Transmittance and absorbance spectra

Measuring the transmittance and absorbance spectra of untreated water PAW-3 and PAW-15 (highest RNS, and H_2O_2, respectively) were carried out using double-beam UV-vis-NIR spectrophotometers (JASCO V-670) following the procedures published by (Oh et al., 2018) to determine the differences between PAW-3 and PAW-15. Quartz cuvettes with a constant spectral resolution of 0.2 nm, and a constant scan speed of 120 nm/min were used for the measurements. Five minutes following the PAW preparation, the measurements were made [20].

2.3. Statistical Analysis

SPSS software (version 16.0, IBM, Chicago, IL, USA) was used to analyze statistics. Due to the small sample size (The experiments were replicated three times, n=3), Kruskal Wallis nonparametric analysis was used to assess statistical differences, followed by the Mann-Whitney test, With $p < 0.05$ as the significant level.

3. Results and Discussion

The study findings suggest that the CAP application for water treatment leads to a notable alteration in the properties of the liquid media. It is worth noting that previous long-term research in various scientific domains has already highlighted the effectiveness of PAW, including our contribution to the field.

3.1 Current-voltage waveform plasma discharge

In Fig. 4, the voltage and current waveform show that the discharge type is a spark. the voltage oscillates with exponentially decaying amplitude, and the current oscillates similarly. Spark discharge is characterized by the higher current in our current values. A spark is formed when the high voltage applied to the electrode is increased; an ionized channel is formed between the two electrodes, and a filamentary streamer transmits to the spark [21-22].

A typical emitted spectrum of air discharge from the plasma reactor has been noted and is depicted in Figure 5. The wavelength range is 300-400 nm, with dominant emitted spectra corresponding to the nitrogen second positive system (N^2 2P system) bands at 313.6, 337.1, 353.6, 357.6, 375.5, and 380.49 nm [23].

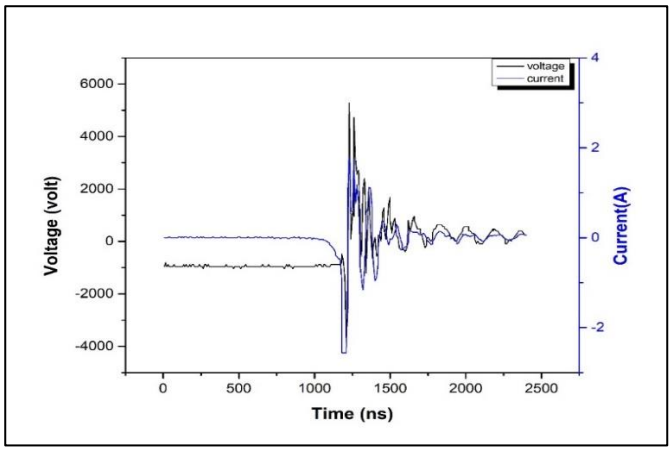

Figure 4: Current-voltage waveform plasma discharge in air at 5 kV applied voltage.

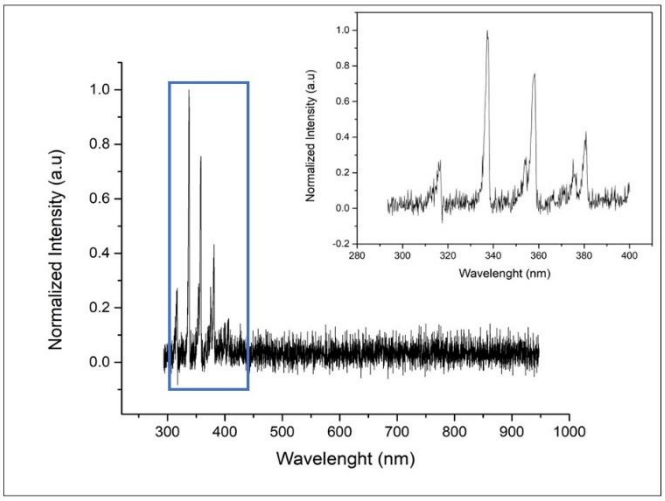

Figure 5: The optical emission spectrogram depicts the operation of the spark plasma system in atmospheric air.

3.2 Temperature, EC, and pH

Fig. 6 (a, b, and c) displays the temperature, EC, and pH values of DW and PAW. When subjected to plasma activation, DW experiences a gradual increase in temperature. Initially, the water is at room temperature (28.45 °C) but after 3 minutes of plasma exposure, the temperature increases by 4.05 ± 0.25°C. Following 15 minutes of plasma exposure, the temperature rises by 9± 0.2°C, corresponding to an absolute temperature of 32.5 ± 0.6°C and 37.45 ± 0.15°C, respectively. However, the heating process is not linear, and after 10 minutes of activation, the rate of temperature increase slows down, and the water's temperature reaches a plateau estimated at 37.18± 0.10°C. This behavior is

consistent with previous findings reported by Judée et al. [24], who suggested that the temperature plateau noted during extended exposure of liquid media to plasma suggests a balance between the plasma source and the liquid temperature. According to Chou et al. [6] the rise in temperature could be attributed to the production of plasma beams, which are accompanied by thermal energy. This energy tends to accumulate over time in the PAW. Mahdikia et al. [8] observed that after six minutes of plasma treatment, water temperature increased linearly up to 33.8 °C.

Fig. 6 (b) recorded an increase in EC from 18.72 in DW to 163.8 (µS/cm) in PAW-15, which can be ascribed to the production of reactive oxygen species (ROS) and reactive nitrogen species (RNS) in PAW. Mahdikia et al. [8] identified the production of H^+ ions as the primary cause of the altered electrochemical properties of water subjected to a cold plasma jet treatment. After six minutes of plasma treatment, they observed an increase in EC from 3.16 µS/cm to 102.36 µS/cm and the water temperature increased linearly up to 33.8 ºC. Similar findings have been reported in other studies, wherein the EC was observed to significantly increase. This may be explained by the presence of ROS, including O_3, O^-, O, OH·, and other substances, which are more abundant in PAW. These substances are highly unstable and possess potent oxidizing properties, and they dissolve in water in large quantities during exposure to plasma, resulting in an elevation of EC [6]. Yang et al. [4] investigated the EC variation in PAWs; they revealed a drastic increase in EC within a 5-minute timeframe. This notable increase was primarily attributed to the generation of active substances, such as ROS and RNS, which are formed when air is ionized and dissolved in water. The persistent rise in EC observed during plasma activation suggests the production of active ions within the water [5] Fig. 6 (c) showed that the pH of PAW significantly decreased from 7 to 3.66 within 15 minutes of cold plasma treatment, which aligns with prior research outcomes [25]. Mahdikia et al. [8] recorded that after six minutes of plasma exposure, they noted a reduction in pH levels from 7 to 3.25. They explained that using air for producing PAW leads to the generation of reactive species, such as hydroxyls (OH.), nitrate (NO_3^-), and nitrites (NO_2^-), which results in the production of hydrogen peroxide (H_2O_2), nitric acid (HNO_3), and peroxynitrous acid, causing PAW to become acidic.

Yang et al. [4] noticed that the pH of the PAW dropped as the treatment duration increased. This pH decrease was a result of water ionization, resulting in the generation of H+ ions and acidic compounds such as nitric acid and nitrous acid. Vaka et al. [26] noted a more pronounced decrease in pH during briefer exposure periods (5 to 12.5 minutes). However, no notable distinctions were observed between the 12.5 and 20 minutes of exposure. Researchers found that throughout the exposure period, RNS and ROS from the atmospheric pressure plasma discharge dissolved or diffused into the water. These substances then interacted with molecules of water, causing a multitude of chemical species to be produced. The pH decreased because of the discharge of hydrogen ions that coincided with the creation of these chemical species.

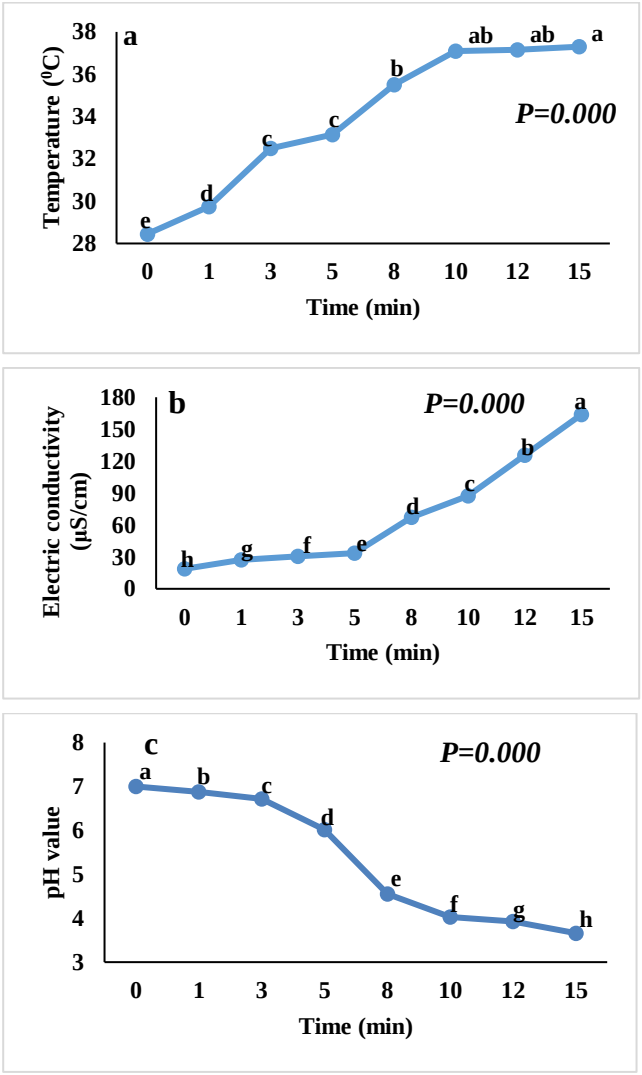

Figure 6: (a-c): PAW (a) temperature, (b) Electrical conductivity (EC), and (c) pH reliance on the treatment duration for 100 ml water samples. Data was collected directly after plasma exposure. Line markers with different a-h superscripts are significantly different.

The study documented a pH reduction of up to 2.4 ± 0.1, which varied based on the specific operating environments. As a result of gas-phase interactions involving dissociated N_2 and O_2, nitrogen oxides (NO_x) generated in the air plasma dissolved, forming nitrites and nitrates in PAW. The pH decrease was partly caused by ions of hydrogen (H^+) that were produced when NOx dissolved in water. Additionally, the study found that H_2O_2 was formed in the PAW through the recombination reaction of hydroxyl radicals ($OH^•$) produced by the plasma at the interface between the gas and liquid phases. This production of H_2O_2 further contributed to the observed pH decrease in the PAW. After being treated with plasma, the DW water became acidic. Chen et al., [27] ascribed the acidification of PAW to RNS generated by plasma, including nitrate and nitrite, as well as hydrogen cations resulting from the dissociation of water molecules.

3.3 Contact Angle

The PAW contact angles measured at different exposure

times were presented in Fig. 7. The outcomes demonstrated that as exposure time rose, the PAW contact angles decreased, resulting in smaller contact angles than those of DW droplets. At 15 minutes of exposure, the contact angle of PAW was reduced by an average of 20.5°, or 40.26%, compared to DW, which had a contact angle of 34.32°. This suggests that when treated water and the glass surface interact, plasma raises the surface energy. Similarly, Shaji et al. [12], demonstrated that at ambient temperature, the contact angle of DW droplets on glass surfaces is lowered upon exposure to air plasma. However, the measured contact angle for DW in their study was 54.5°, whereas, in the current study, the contact angle was found to be 34.32°. This discrepancy in the measured contact angle could potentially be attributed to differences in the experimental conditions between the two studies, such as the room temperature during the measurements. The Shaji et al., [12] study was conducted at 18°C and the current study at 29°C. An effective measure of the cohesive and adhesive forces of a liquid is its contact angle, with a lower angle indicating higher wettability and adhesion [12]. These findings imply that liquid plasma activation could be beneficial for improving the adhesion and wettability of paints, dyes, and other materials used in the surface treatment industry.

3.4 Concentration of H_2O_2 and NO_2^-

During the process of CAP water treatment, several long-lived RNS and ROS compounds were observed to appear in the liquid media, including NO_2^-, NO_3^-, O_2, H_2O_2, and others [28]. As shown in Fig. 8 (a), the H_2O_2 concentration rose about linearly with treatment duration, with the density of H_2O_2 reaching about 0.22 mM/L in PAW-15. H_2O_2 is formed by the recombination of OH radicals. The duration of plasma exposure is directly correlated with the amount of H_2O_2 generated in PAW, as shown in Fig. 8 (a). This relationship is comprehensible given that longer plasma exposure times result in greater accumulation of reactive species such as hydroxyl radicals (•OH), H_2O_2, and other plasma-derived molecules.

As the DW is continuously exposed to plasma discharge and gas flow, water evaporation increases, leading to the enhanced generation of H_2O_2 through reactions [29]. In the research carried out by Yang et al. [4] the concentration of H_2O_2 in PAWs was examined about treatment time. The results revealed that by prolonging the treatment duration, there was a noteworthy elevation in the concentration of H_2O_2. Specifically, after 5 minutes of treatment, the H_2O_2 concentration reached 5372.69 µmol/L, demonstrating an approximately 110-fold increase compared to the concentration observed at 1 minute.

As shown in Fig. 8 (b), The concentration of nitrite ions (NO_2^-) exhibited a peak at PAW-3, reaching a maximum of 96.26 µM/L, followed by a subsequent decline to 2.57 µM/L at PAW-15 Similarly, Wang & Salvi,[5] reported that the reaction between these RNS substances and the hydroxide ions and water led to the progressive accumulation of nitrite (NO_2^-) in the solution. The NO_2^- concentration commenced a decline after attaining a peak value of 2.6 ± 0.2 mmol/L at 5 minutes, reaching 2.0 ± 0.1 mmol/L at 15 minutes. This pattern suggests the probable conversion of NO_2^- into other RNS. Ma et al., [30] attributed the decline of NO_2^- in PAW to the transformation of NO_2^- into the unstable HNO_2, which subsequently decomposed into NO, NO_3^-, and ONOO. Also, Takahashi et al., [31] showed that when specific energy increases, the NO_2^- concentration in the pulsed plasma discharge first rises and subsequently falls. On the contrary, according to Yang et al. [4], the concentration of NO_2^- showed a steady increase during the experiment. This increase was primarily attributed to the reaction between RNS substances, such as NO, NO_2, and others, which are produced when ionized air dissolves in water, with OH^- (hydroxide ions) and H_2O. Mizoi et al. [32] suggest that substantial quantities of H_2O_2 and NO_2 were generated within the initial 60 minutes of treatment. As the treatment progressed, it became evident that NO_2 was undergoing oxidation by H_2O_2, resulting in the production of significant amounts of nitrate ions (NO_3). Given H_2O_2's robust oxidizing properties in acidic environments, it was anticipated that H_2O_2 would function as an oxidizer within the PAW system. Essentially, H_2O_2 began operating as an oxidant as the pH decreased with the prolonged treatment duration.

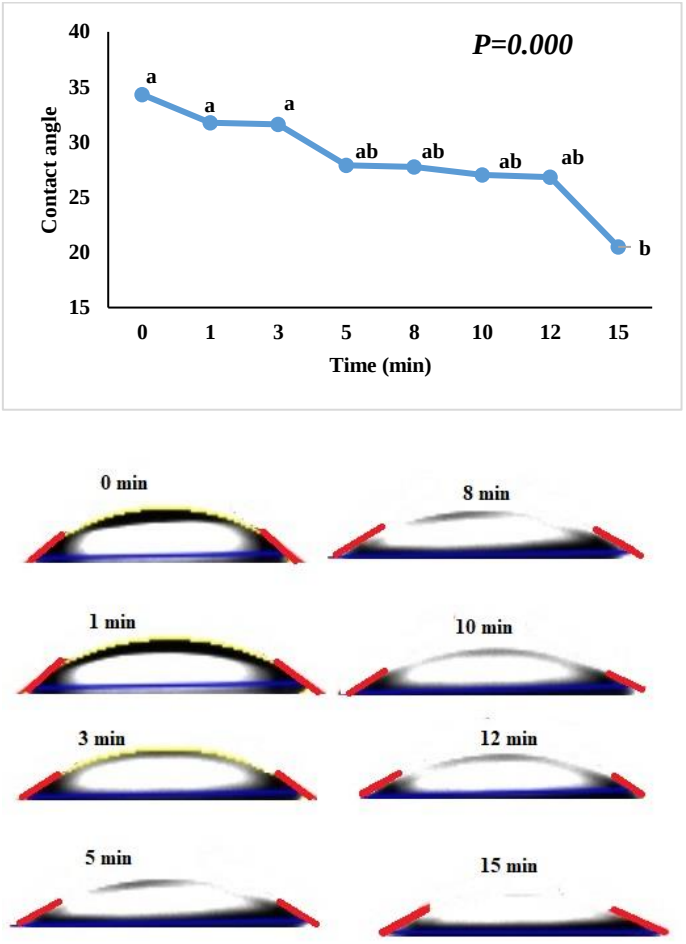

Figure 7: PAW contact angle reliance on the treatment duration for 100 ml water samples. Data was collected directly after plasma exposure. Line markers with different [a-b] superscripts are significantly different.

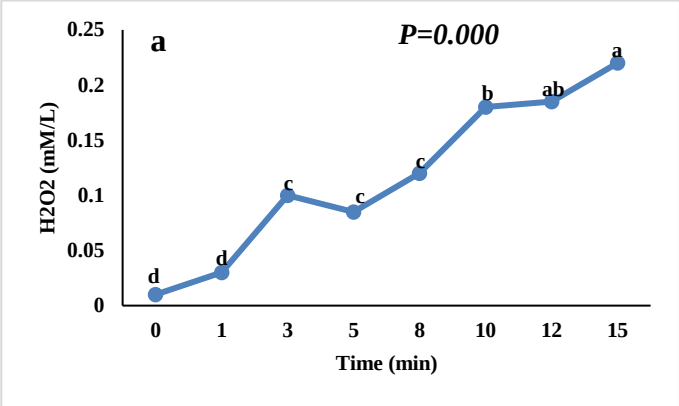

Figure 8 (a, b): PAW (a) hydrogen peroxide and (b) nitrite concentration reliance on the treatment duration for 100 ml water samples. Line markers with different [a-c] superscripts are significantly different.

3.5 Transmittance and absorbance spectra

In Fig. 9 (a), the transmittances for DW, PAW-3 and PAW-15 were determined using the JASCO V-670 spectrophotometer across a wavelength range of 200–2500 nm. The UV–vis–NIR spectra were nearly indistinguishable within the 340–2500 nm range in DW and PAW-3min samples. However, below 340 nm, the spectra diverged. Conversely, below 1136 nm, differences were observed between DW and PAW-15min. This variation is attributed to the different concentrations of ROS, RNS and O_2 in PAW compared to those in DW, as documented by Oh et al. [20]. Consequently, subsequent measurements were focused on shorter wavelengths (190-340 nm). Fig. 9 (b) illustrates the typical spectra of PAW-3 and PAW-15. As anticipated, the intensity of the absorption spectra demonstrated an augmentation with an increase in plasma exposure time. Although the profiles of the spectra bore a resemblance, they were not identical. A detailed analysis revealed a minor shift in the central peak position from 208 nm following 3 minutes of plasma exposure to shorter wavelengths after prolonged exposure (194 nm at 15 minutes). These subtle variations in peak profiles imply that alterations occurred not only in the concentration of ROS, RNS, and oxygen (O_2) with plasma exposure but also in the composition of RNS present in PAW [20]. The absence of absorption in the 200-220 nm range may be linked to electronic transitions or structural alterations within the NO2 molecule induced by the experimental conditions. Our chemical analysis revealed that the concentration of NO_2 is lower in PAW-15 when compared to PAW-3.

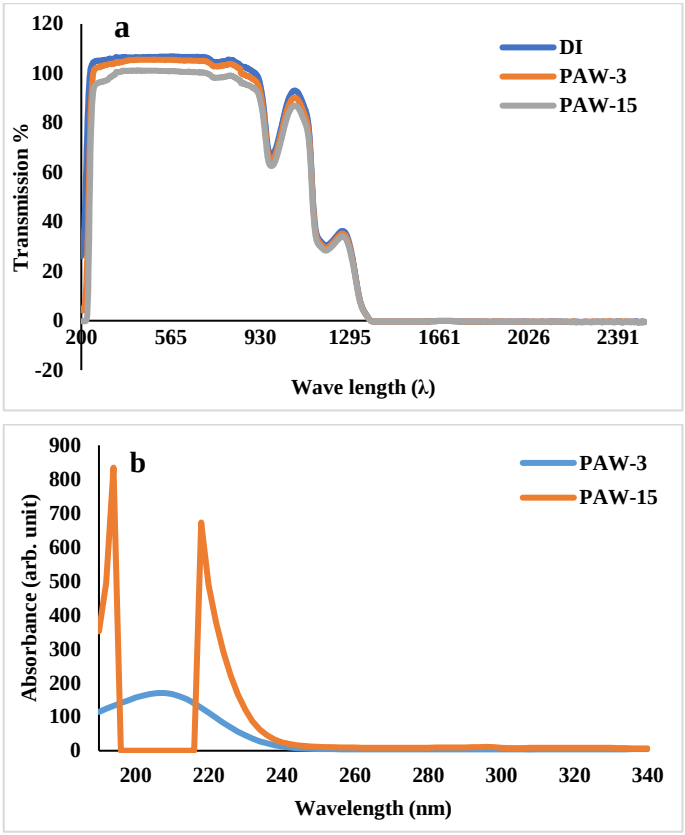

Figure 9: PAW (3 and 15 min) transmission spectra

3.6 Storage

The storage stability of PAW remains unclear and even contradictory [33]. The stability and biological activity of the PAW are significantly influenced by the storage temperature and duration, as well as the initial PAW chemistry and generation conditions [26]. The current study reported no significant changes in pH, EC, and concentrations of H_2O_2 and NO2 in PAW stored for 20 days at -20 0C, as shown in Fig. 10 (a-d). Similarly, Vlad & Anghel, [34] demonstrated very small variations of the physicochemical properties of PAW including pH and EC, concentrations of H_2O_2, and NO_3^- over 3 weeks of storage at room temperature. Vaka et al., [26] revealed that after two weeks of cold storage, the measured pH, nitrates, and nitrites levels stayed constant (no statistically significant variations). The average nitrate/nitrite levels did, however, show a modest increase/decrease, which is explained by the acidic pH of PAW, which causes nitrites to break down into nitrates and nitrogen oxide. On the contrary, several research studies reported significant changes in PAW after storage. The observed change in the physicochemical properties of PAW is less than 10% for two-week storage at 4 °C by Rathore & Nema [9]. Similarly, NO_3^- and H_2O_2 concentration changes lies within 5% and 1.54%, respectively. However, the NO_2^- and dissolved O_3 concentrations fall significantly during the storage period. Tsoukou et al. [35] unveiled that the impact of storage

temperature on preserving the bactericidal activity of PAW followed the order of RT < 4 < −16 < −80, equivalent to −150 °C (where storage at −80 and −150 °C exhibited similar preservation effects). Storing non-buffered PAL at −80 °C or −150 °C proves to be an effective method for maintaining their bactericidal activity during prolonged storage, emphasizing the need for caution when using conventional freezers over the extended storage period. Wang & Salvi, [5] suggested that storage conditions can affect the PAW physical-chemical characteristics and should be considered in its use. Their results showed no significant changes in pH, ORP, EC, and NO_3^- concentration during the one-hour storage of PAW. However, a significant decrease in the concentration of NO_2^- was reported, which was associated with the decline in PAW effectiveness during storage. During a 48-hour storage period at either room temperature or 4°C, no noteworthy pH, ORP, or EC alterations were detected, However, there was a swift reduction in NO_3^- concentration, with a more gradual decline at 4°C in comparison to room temperature. Similarly, the NO_2^- concentration exhibited a notable decrease during storage at both temperatures. An investigation evaluating the bactericidal effectiveness of PAW against Staphylococcus aureus considered various PAW storage conditions (−80, −20, 4, and 25 °C, for up to 30 days). The findings indicated that the concentrations of reactive species in PAW, including hydrogen peroxide, nitrites, and nitrates, diminished with prolonged storage time. Moreover, this reduction was more conspicuous at elevated storage temperatures [7]. Traylor et al. [14] have also evaluated PAW's prolonged antibacterial activity after seven days of storage at an undisclosed temperature. The pH didn't change during the entire period, but the levels of hydrogen peroxide and nitrites dropped below the detection limit in two days, while the levels of nitrate rose quickly at first and more slowly over the next four days. On the contrary, Niquet et al.[36] have found that following a 24-hour storage period at 4 °C, there is a rise in the concentration of hydrogen peroxide and a corresponding amount of nitrates; nitrites were not found either before or after storage.

4. Conclusion

In conclusion, our study focused on investigating the properties of DW treated with air plasma. We found that the treated water predominantly contains RNS, and ROS species specifically NO_2^- and H_2O_2, which can be stored for at least 20 days at -20 OC without significant alterations in concentration. The EC of the treated water increases linearly with treatment time, while the pH decreases with exposure time. Our findings align with previous research in this field. Our study provides valuable insights into the potential uses of PAW for different objectives, including biomedical research, food preservation, and improving the quality of planting materials. Additionally, this energy-efficient technology offers an effective solution for creating PAW of different natures, presenting a promising area for further exploration and innovation.

Acknowledgments

This study was partially supported by Sohag University and Assiut University.

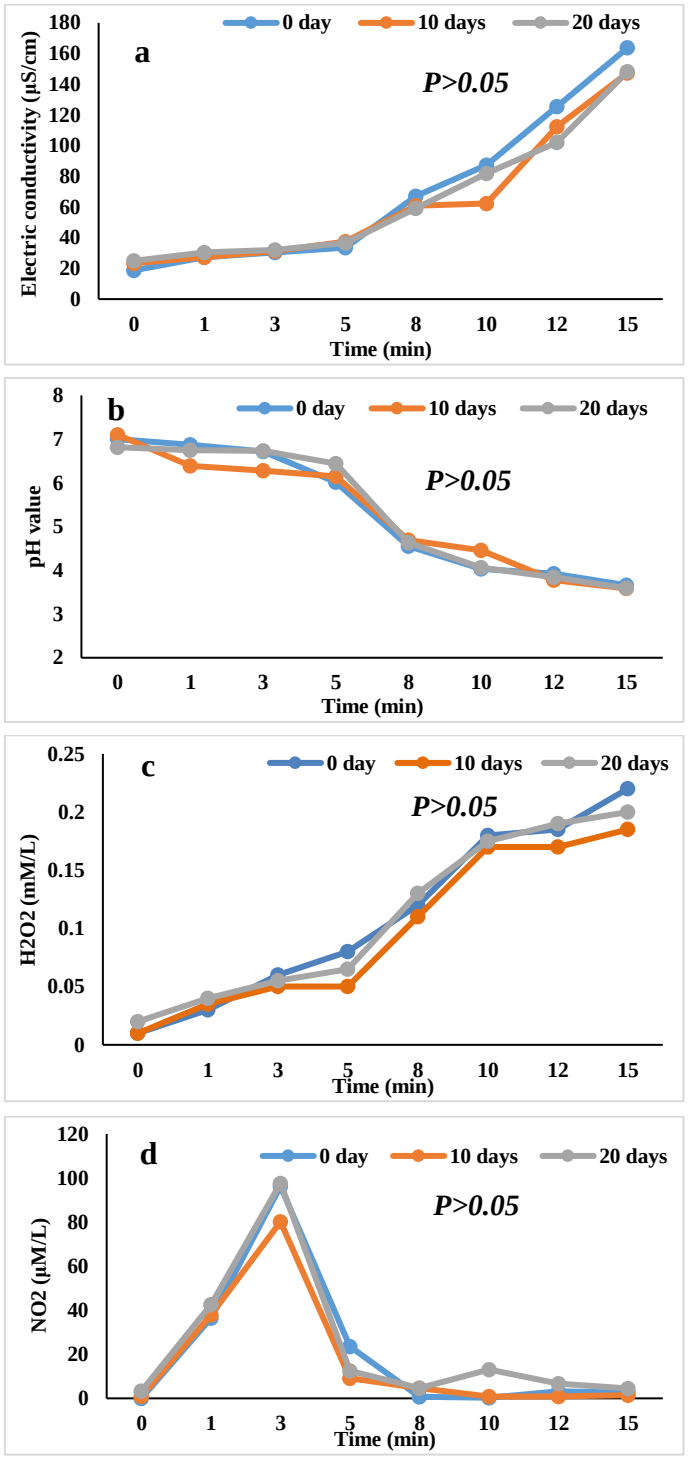

Figure 10 (a-d): (a) Electrical conductivity (EC) and (b) pH (c) hydrogen peroxide and (d) nitrite concentration reliance on the on-storage duration.

Declaration of originality

We hereby declare that the article presented is original and has not been published or under review for publication elsewhere. Additionally, all figures included in the article are our own original work, and no permission is required for their use.

CRediT authorship contribution statement:

FH and MM developed the concept and methodology, wrote the proposals, and led the research team. GA, MK, and AS worked on the electrical characterization of the plasma circuit and all other experimental work. The whole team participated in the manuscript's drafting and review process. Each author carefully read and approved the document.

Data availability statement

The data utilized to substantiate the conclusions of this study can be obtained by reaching out to the corresponding author upon request.

Declaration of competing interest

The authors assert that they do not have any known conflicting financial interests or personal relationships that might have been perceived to influence the work documented in this paper.

References

[1] S. Kim, C. H. Kim, *Biomedicines*, 9(2021), 1700.
[2] D. Guo, H. Liu, L. Zhou, J. Xie, C. He, *J Sci Food Agric*, 101(2021) 4891–4899.
[3] S. Meropoulis, C. A. Aggelopoulos, *J Environ Chem Eng*, 11(2023) 109855.
[4] X. Yang, C. Zhang, Q. Li, J.-H. Cheng, *Molecules*, 28(2023).
[5] Q.Wang, D. Salvi, *LWT*, 149(2021).
[6] Y.-J. Chou, Y. Tseng, K. C. Hsieh, Y. Ting, *Food Biosci*, (2023), 102613.
[7] J. Shen et al., *Sci Rep*, 6 (2016).
[8] H. Mahdikia, B. Shokri, K. Majidzadeh-A, *Iranian Journal of Pharmaceutical*, 20(2021)
[9] V. Rathore and S. K. Nema, *J Appl Phys*, 129(2021).
[10] H. B. Baniya et al., *J Chem*, 2021(2021) 1–12.
[11] S. Ikawa, A. Tani, Y. Nakashima, and K. Kitano, *J Phys D Appl Phys*, 49(2016).
[12] M. Shaji, A. Rabinovich, M. Surace, C. Sales, A. Fridman, Plasma, 6(2023) 45–57.
[13] I. M. Piskarev, *High Energy Chemistry*, 53(2019) 82–86.
[14] M. J. Traylor et al., *J Phys D Appl Phys*, 44 (2011).
[15] P. Lu, D. Boehm, P. Bourke, P. J. Cullen, *Plasma Processes and Polymers*, 14(2017).
[16] Y. Gorbanev, A. Privat-Maldonado, A. Bogaerts, *Analytical Chemistry*, 90(2018) 13151–13158.
[17] J. L. Brisset and J. Pawlat, *Plasma Chemistry and Plasma Processing*, 36(2016)355–381.
[18] P. Lukes, E. Dolezalova, *I. Sisrova, and M. Clupek, Plasma Sources Sci Technol*, 23(2014).
[19] S. Herianto, C. Y. Hou, C. M. Lin, H. L. Chen, *Comprehensive Reviews in Food Science and Food Safety*, 20(2021)
[20] J. S. Oh et al., *Jpn J Appl Phys*, 57(2018).
[21] M. Janda, V. Martišovitš, Z. Machala, *Plasma Sources Sci Technol*, 20(2011).
[22] N. L. Aleksandrov , E. M. Bazelyan, *Plasma Sources Sci Technol*, 8(1999).
[23] P. Jitsomboonmit, M. Nisoa, S. Dangtip, *Physics Procedia*, 32(2012).
[24] F. Judée, S. Simon, C. Bailly, T. Dufour, *Water Res*, 133(2018)47–59.
[25] A. Y. Okyere, P. G. Boakye, E. Bertoft, G. A. Annor, *Curr Res Food Sci*, 5(2022)1668–1675.
[26] M. R. Vaka et al., *Foods*, 8 (12), (2019).
[27] Z. Chen, Y. E. Krasik, S. Cousens, A. T. Ambujakshan, C. Corr, X. J. Dai, *J Appl Phys*, 122(2017).
[28] E. M. Konchekov et al., *Front Phys*, 8(2021).
[29] B. Ghimire et al., *Plasma Sources Sci Technol*, 30(2021).
[30] M. Ma, Y. Zhang, Y. Lv, F. Sun, *J Phys D Appl Phys*, 53(2020).
[31] K. Takahashi et al., *Jpn J Appl Phys*, 55(2016).
[32] K. Mizoi et al., *RSC Adv*, 12 (2022)7626–7634.
[33] S. Perinban, V. Orsat, V. Raghavan, *Comprehensive Reviews in Food Science and Food Safety*, 18(2019).
[34] I. E. Vlad, S. D. Anghel, *J Electrostat*, 87(2017).
[35] E. Tsoukou, P. Bourke, D. Boehm, *Water (Switzerland)*, 12(2020)1–18.
[36] R. Niquet, D. Boehm, U. Schnabel, P. Cullen, P. Bourke, J. Ehlbeck, *Plasma Processes and Polymers*, 15(2018).